ELSEVIER

Journal of Hazardous Materials B136 (2006) 902–910

Journal of Hazardous Materials

www.elsevier.com/locate/jhazmat

Photocatalysis of 2,2′,3,4,4′,5′-hexachlorobiphenyl and its intermediates using various catalytical preparing methods

Y.J. Lin *, Y.L. Chen, C.Y. Huang, M.F. Wu

Department of Environmental Science and Engineering, National Pingtung University of Science and Technology, Pingtung, 912, Taiwan

Received 9 September 2005; received in revised form 18 November 2005; accepted 16 January 2006
Available online 21 February 2006

Abstract

Four etching solutions used on support materials and two coating methods of TiO_2 were conducted to investigate the effects of catalytical preparing methods on the photocatalysis of 2,2′,3,4,4′,5′-hexachlorobiphenyl (PCB congener 138). The results of XRD analyses confirmed that various etching solutions used on support substrates did not influence the characteristics of titanium(IV) oxide. The XRD patterns of crystallization for the catalysts before and after purification remained unchanged. Hydrofluoric acid used as an etching solution for the support substrates provided the best adhesion stability for the catalysts that demonstrated the highest photocatalytic efficiency for congener 138. Xenon and ultraviolet lamps were used to compare the irradiation effect on photocatalysis. The shortest half-lives of congener 138 were 7.4 and 12.2 h using xenon and UV reactors, respectively. Lower chlorinated biphenyls (lower congener numbers) were identified through the continuous dechlorination of congener 138. PCB congeners 99, 87, 66, 49, 28, 17, 9, and 7 were detected as a result of dechlorination from higher chlorinated congeners to lower chlorinated congeners along with the extension of exposure times. The concentrations of chloride ion were increased with increasing exposure time through dechlorination, while the concentrations of organic chlorine of congener 138 were decreased. Meta-dechlorination was the most commonly found mechanism for the photocatalysis of PCB 138. The activation energy of the photocatalysis of congener 138 was 70.8 kJ mol^{-1}.

Keywords: PCBs; Congener 138; Dechlorination; Etching; Coating; TiO_2

1. Introduction

The deterioration of environmental quality has raised serious safety concerns due to the release of industrial wastes such as polychlorinated biphenyls (PCBs). Estimated 30 metric tons of PCBs have been released to the nature and became a ubiquitous contaminant worldwide, mostly in sediments [1,2]. More than one billion dollars has been spent on the clean up of PCBs contamination with limited progress [3]. In 1979, more than 2000 people were poisoned through the consumption of PCBs contaminated rice oil in Taiwan. The chronic toxic effects of PCBs include failure of reproduction, birth defect, and brain damage. Some PCB congeners have the similar structure as 2,3,7,8-tetrachlorodibenzodioxin (TCDD); thus, their toxic properties are similar to that of TCDD. Aroclor® 1254 was one of the most commonly used industrial PCB fluids. There are 37 congeners (each at greater than 0.5% by weight) that can be found in Aroclor® 1254. Congener 138 (2,2′,3,4,4′,5′-hexachlorobiphenyl) is one of the major congeners that accounts for 9.1% of the total mass of Aroclor® 1254.

Photodegradation is one of the most natural decomposition mechanisms for PCBs [4–12]. However, most PCB congeners do not strongly absorb the wavelength above 380 nm. Indirect photodegradation can be greatly enhanced through the use of photocatalysts or photosensitizers by exposure to light energy. Photocatalysis such as using titanium(IV) oxide has been proved to be an effective mechanism for the degradation of environmental contaminants [13–18]. Titanium(IV) oxide including three polymorphs of anatase, rutile, and brookite is commonly used to enhance the quantum yields of photocatalyses [16]. Apparent quantum yield is calculated as the ratio between the amount of reactant degraded and the amount of quantum emitted [19].

Advanced oxidation processes (AOPs) that involve light-induced redox reactions are able to generate highly reactive intermediates such as hydroxyl radicals ($^{\bullet}OH$) and superoxide

* Corresponding author. Tel.: +886 8 774 0470; fax: +886 8 774 0256.
E-mail address: yjlin@mail.npust.edu.tw (Y.J. Lin).

0304-3894/$ – see front matter © 2006 Elsevier B.V. All rights reserved.
doi:10.1016/j.jhazmat.2006.01.031

ion ($^{\bullet}O_2^-$) to initiate a sequence of decomposition reactions for PCBs

$$TiO_2 + hv \rightarrow TiO_2^*(h^+_{vb} + e^-_{cb})\ E_{bg} = 3.2\,eV,$$

$$h^+_{vb} + H_2O_{(ads)} \rightarrow {}^{\bullet}OH + H^+$$

Two most commonly selected light sources, UV and xenon lamps were applied on the related investigations. UV lamps provide most light energy in a single line spectrum such as 254 nm that can be strongly absorbed by most xenobiotics including PCBs. As a result, UV lamps are the most commonly chosen light source on AOPs studies. Contrarily, xenon lamps provide wavelengths ranged between 150 and >900 nm which is similar to that of natural sunlight (120 ~ > 1000 nm). Most xenon photoreactors are used to simulate natural sunlight to investigate the mechanism of solar degradation for pollutants. The most important advantage of using solar energy is because it is one of the few energy sources having no detrimental impact on the environment.

Percent degradation, degradation rate, rate constant, and half-life were the most common ways to present the results of photocatalytical studies [10–12,20,21]. However, because of different experimental settings applied, those data were not practically to be evaluated among each other on the efficiency of photocatalyses. Apparent quantum yields were calculated as the ratio between the amount of reactant degraded and the amount of quantum emitted [8,19,22,23]. It can be used to compare the photocatalytic efficiencies of pollutants present in aquatic systems [22].

Both titanium(IV) oxide and titanium(IV) tetraisopropoxide ($Ti(OC_3H_7)_4$) have been applied in the homogeneous (suspension state) or heterogeneous solutions (coated onto support materials such as glass substrates) [24,25]. The aqueous system of photocatalytic suspension, an effective design for the degradation of xenobiotics, can be readily prepared with the drawback of difficulty to recover the suspended catalysts. To compensate this disadvantage, catalysts can be immobilized by coating onto the surface of glass substrates as a stationary phase [13]. Titanium(IV) oxide particles can also be attached to silica gel on sol–gel [16]. Poor adhesion of catalysts on support substrates is a common problem existed in the research using immobilized photocatalysts. Various etching solutions and processes were practiced to improve the adhesion stability of catalysts on support materials. The objective of this study was to compare the effects of different etching solutions used on glass substrates and TiO_2 coating methods on the photocatalysis of PCB congener 138.

2. Materials and methods

2.1. PCB congener 138

Neat PCB congener 138 (2,2′,3,4,4′,5′-hexachlorobiphenyl) (AccuStandard Inc., Connecticut, USA) was dissolved in acetone to increase its solubility and used as stock solution. Three concentrations of PCB congener 138 were prepared as 0.28, 1.4, and 2.8 μmol L^{-1} (equivalent to 0.1, 0.5, and 1.0 mg L^{-1}, respectively). The percentage of organic chlorine in PCBs can be calculated using the equation below [26]. The ratio of organic chlorine of congener 138 was 58.97%

$$C_{Cl0} = C_{PCBGi} \times N_{ClGi} \times MW_{Cl}/MW_{PCBGi}$$

where C_{Cl0} is the organic chlorine concentration, C_{PCBGi} the PCB concentration of *i*th group (ppm), N_{ClGi} the average number of chlorine atoms of *i*th PCB group, MW_{Cl} the chlorine atomic weight and MW_{PCBGi} is the average molecular weight of *i*th PCB group.

The mixture of 209 pure standard PCB congeners (AccuStandard Inc., Connecticut, USA) was used to verify the degraded intermediates of the photocatalysis of congener 138. The identifications of 209 pure standard PCB congeners were analyzed and confirmed using a HP5995C gas chromatograph–mass spectrometer (GC–MS) equipped with a chemstation (HP 59970). The degraded intermediates of congener 138 photocatalysis were verified by comparing the relative retention times (RRT) and the relative responses (RR) of the pure standard congeners [27].

2.2. Purification of titanium(IV) oxide

Titanium(IV) oxide (Degussa, P-25) (70% anatase, 30% rutile) and titanium(IV) tetraisopropoxide ($Ti(OC_3H_7)_4$) were purchased from Sigma–Aldrich and Merck, respectively. The pH of titanium(IV) oxide suspension was adjusted to two using 0.2 M $HClO_4$. The upper clear layer of the solution was discarded. Distilled water was added to wash the TiO_2 solution and then discarded. The procedure was repeated until the pH of TiO_2 solution reached 7. The solution of TiO_2 was then placed in a reverse osmosis system until the conductivity of solution was closed to that of distilled water. Finally, the TiO_2 suspension was dried at 103 °C until its weight remained constant. The purified TiO_2 sample was then ground prior to coating onto glass substrates. Both TiO_2 with and without purification were compared to investigate the effect of purification on the photocatalysis of congener 138.

2.3. Etching and coating processes

Glass substrates (3 mm) were used as the support materials for TiO_2. Four etching solutions (listed as G1, G2, G3, G4) were prepared to create a rough surface of support materials to improve the adhesion stability for TiO_2. Sodium hydroxide (5 M) and hydrofluoric acid (48%) were used to etch the 3 mm glass substrates at 100 °C labeled as G1 and G2, respectively. A mixed solution (7:3 v/v) of sulfuric acid and hydrogen peroxide was used as G3 at 90 °C. The etching solution of G4 was prepared using a mixed solution of HF (48%), H_2O_2 (30%), and NH_3 (29%). Etched glass substrates were coated with titanium(IV) oxide (1 or 5 wt.%) at 105 °C for 2 h. The coating process was repeated twice.

The other coating method was conducted using the sol–gel method. Zeolites and glass substrates were chosen as support materials. Titanium(IV) tetraisopropoxide ($Ti(OC_3H_7)_4$) was dissolved in the mixed solution of ethanol, distilled water and

nitric acid for 8 h [25]. Zeolites were added to the solution and dried at 50 °C for 3 h and then at 120 °C overnight. The final calcination temperature was 450 °C in an oven for 12 h [28]. For the other preparing method, titanium(IV) tetraisopropoxide was dissolved in ethanol overnight. Glass substrates were submerged and then removed out of the solution at the speed of 2.3 cm min^{-1}. Glass substrates were then calcined at 400 °C for 2 h.

2.4. Irradiations

PCB samples placed in quartz vessels were exposed to a 150 W xenon lamp (L2274, Hamamatsu Photonics, Japan) and a 35 W UV lamp with the major spectrum of 254 nm (RPR-200 Rayonet, USA) (Fig. 1). The radiant energy (mW cm^{-2}) and luminous flux (Foot-Candle, Ft-cd) of both light sources were measured by a LI-250 light meter equipped with a LI-190SA pyranometer sensor (LI-COR Inc., Nebraska, USA) and a LX-105 light meter (Lutron Inc., Taiwan), respectively. Four exposure times used were from 0, 8, 16 to 32 h. The temperatures of the reaction chambers and reactor vessels were also monitored.

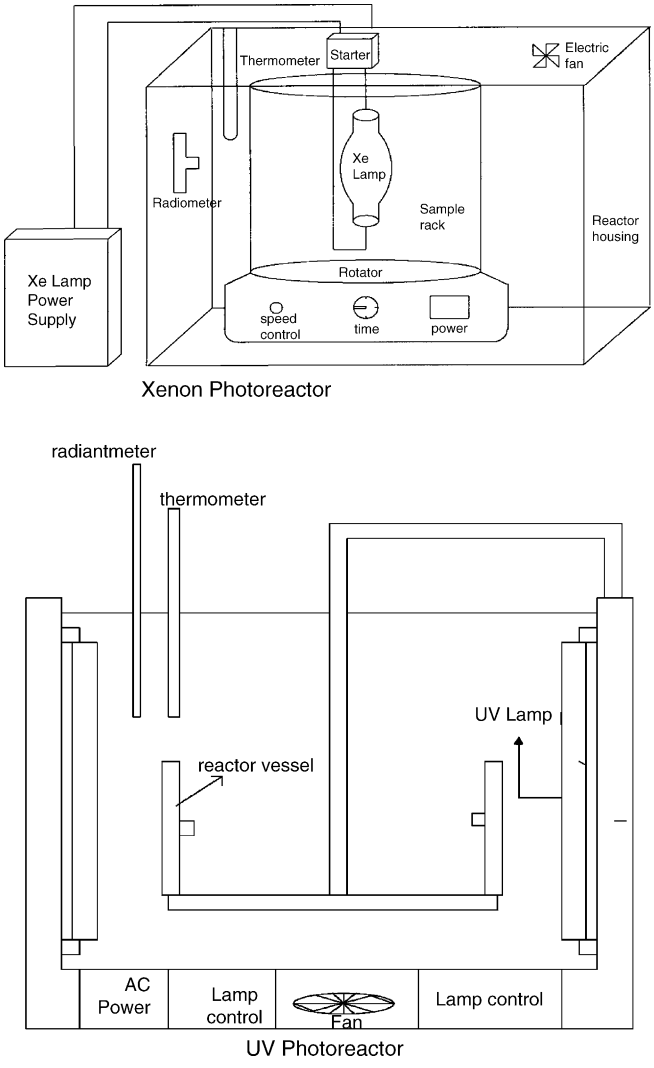

Fig. 1. Schematic drawings of xenon and ultraviolet photoreactors.

For quality control, the experiments were conducted in three replicates. To study the effect of increasing temperature while exposed to irradiation, samples covered with aluminum foil were exposed to the xenon and UV lamps. Samples without the catalyst were also used to investigate the effect of direct photodegradation of PCB congener 138. Another set of samples was placed in dark to determine the amount of PCB congener 138 been absorbed by the catalyst.

2.5. Analytical methods

BET multipoint method was used to measure the specific surface areas of photocatalysts using a SA3100, Beckman Oulter. After coated onto glass substrates the compositions of TiO_2 were determined by X-ray diffraction (XRD) patterns using a RINET 200 XRD (Rigaku, Japan). The crystalline particles of titanium(IV) oxide with and without purification were also compared using their relative intensities of XRD patterns.

Chrysene-d_{12} was added to hexane solvent prior to the extraction of congener 138 acted as an internal standard to compensate the loss of sample during extraction and analysis [29]. The extraction was conducted using an orbital shaker at 280 rpm for 6 h, and the extraction procedure was repeated once. PCB congener 138 and its degraded intermediates were analyzed using a gas chromatograph equipped with an electron capture detector (GC–ECD) (HP 6890). A HP 5, 30 m (id = 0.32 mm) column (0.25 μm film thickness) was used for analyses. Helium gas was used as carrier gas. The oven temperature was set at 170 °C initially for 1 min, then to 230 °C at 5 °C min^{-1}, then ramp to 280 °C at 3 °C min^{-1} with the final holding time of 5 min. The temperatures of injector and detector were set at 250 and 280 °C, respectively. The amount of sample injected was 1 μL with the detection limit of 0.1 ng mL^{-1} for congener 138. The photocatalytical pathways of congener 138 were constructed by the verification of degraded intermediates with 209 pure standard congeners (AccuStandard Inc., USA). The confirmations of their relative retention times (RRT) and relative responses (RR) were performed [19,26]. The amounts of chloride ion that generated from the dechlorination of congener 138 were analyzed using an ion meter (inoLab, WTW, Germany). The minimum detection limit of chloride ion was 0.01 mg L^{-1}.

The overall reaction order of congener 138 photocatalysis was determined using substitution method. After the reaction kinetic of congener 138 photocatalysis was confirmed as first order, the concentrations of congener 138 were presented as $\ln(C_t/C_0)$ where C_t and C_0 were the concentrations at time t and 0 h, respectively. The data of $\ln(C_t/C_0)$ were plotted against exposure times. The half-lives ($t_{1/2}$) of PCB 138 were calculated by the equation of ($t_{1/2} = 0.693/k$) where k is rate constant. Results were analyzed using the analysis of variance (ANOVA) and least significant difference (LSD) to determine the significant differences ($P < 0.05$) among samples using various experimental settings. A statistical software, Statistix® (Win V. 2.0) (Analytical Software, Florida, USA), was used for statistical analyses.

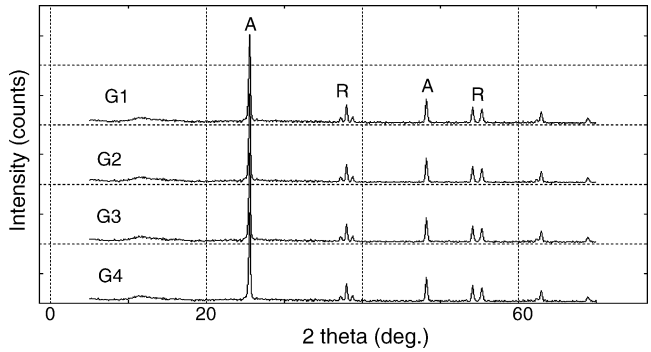

Fig. 2. XRD patterns of unpurified TiO_2 on the support substrates etched by different solutions (G1: 5 M NaOH; G2: 48% HF; G3: H_2SO_4/H_2O_2; G4: $HF/H_2O_2/NH_3$).

3. Results and discussion

3.1. Catalyst characterizations

The specific surface areas of TiO_2 on glass substrates were between 160 and 190 $m^2\ g^{-1}$. The BET of TiO_2 in this study was slightly smaller than those data (188–226 $m^2\ g^{-1}$) reported by Renard et al. (2005) [30]. The results of XRD patterns showed that both rutile ($a = 4.59$ Å, $c = 2.96$ Å) and anatase ($a = 3.79$ Å, $c = 9.51$ Å) phases of TiO_2 were identified in all samples (Fig. 2). Compared the findings of XRD patterns with the data bank of JCPDS cards, the diffractions of anatase (#21-1272) and rutile (#21-1276) of TiO_2 were similar. The peaks of anatase diffraction pattern of TiO_2 at 2θ were 25° and 47–49°. The peaks of rutile diffraction pattern of TiO_2 at 2θ were 37° and 54°. There was no difference in XRD patterns of crystallization among TiO_2 samples using different etching solutions (G1, G2, G3, and G4) on support substrates (Fig. 2). This finding confirmed that four etching solutions did not influence the compositions of P-25 TiO_2. The XRD patterns of catalyst crystallization before and after purification remained the same (Fig. 3). However, significant decrease in relative intensities of both rutile and anatase phases was observed in the samples using titanium(IV) tetraisopropoxide (Fig. 4). The samples using titanium(IV) tetraisopropoxide coated onto zeolite also showed significant decrease in the intensities of rutile and anatase phases. The hydrofluoric acid solution (G2) was used as etching solution for the samples above.

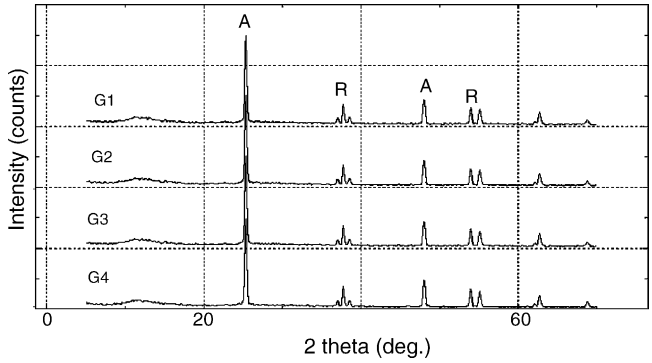

Fig. 3. XRD patterns of purified TiO_2 on the support substrates etched by different solutions (G1: 5 M NaOH; G2: 48% HF; G3: H_2SO_4/H_2O_2; G4: $HF/H_2O_2/NH_3$).

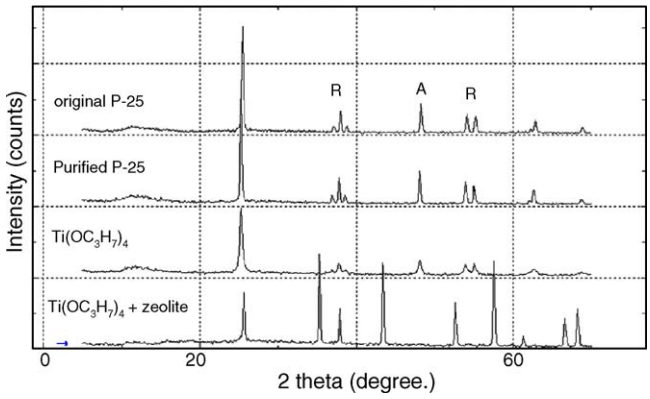

Fig. 4. XRD patterns of TiO_2 (P-25) and $Ti(OC_3H_7)_4$ using different coating methods.

3.2. Radiant energy

The radiant energy of xenon and ultraviolet photoreactors was listed in Table 1. The energy levels of two photoreactors were statistically different from one another. Xenon photoreactor with the light path distance of 15 cm had radiant energy of 39 ± 0.5 mW cm^{-2} (mean ± S.D.). The other group was UV photoreactor with the radiant energy of 4.5 ± 0.1 mW cm^{-2}. The energy levels of xenon and UV photoreactors were equivalent to $(7.8 \pm 0.1) \times 10^{-4}$ and $(9.0 \pm 0.0) \times 10^{-5}$ Einstein $h^{-1}\ L^{-1}$, respectively. The xenon photoreactor had the light energy 8.7 times higher than that of UV photoreactor. By using the formula of ($\ln E_{e,o} = 2 \ln r + \ln E_{e,r}$) [31], the respective surface energy ($E_{e,o}$) of xenon and UV lamps used in this study were 8.7×10^3 and 4.5×10^2 mW cm^{-2} at $r = 0$ cm where r was the distance between the reaction vessel and the lamp. The surface energy of a 450 W mercury lamp was 9×10^3 mW cm^{-2} reported by Doong and Chang (1997) [32]. Under the exposure of xenon and UV lamps, the temperatures of reaction vessels were measured and stabilized at the range of 38 ± 5 and 34 ± 3 °C (mean ± S.D.), respectively.

3.3. Congener 138 photocatalysis

The photocatalytic degradation of PCB congener 138 was increased as a function of irradiation time from 0, 8, 16 to 32 h (Figs. 5–8). Pseudo-first order reaction of congener 138 was confirmed using substitution method. Studies showed that the highest initial degradation rate of congener 138 was the samples using HF (G2) etched support substrate and coated with

Table 1
Energy of irradiation (mean ± S.D.) of xenon and UV photoreactors

Reactors	mW cm^{-2}	Einstein ($L^{-1}\ h^{-1} \times 10^{-4}$)	Wavelength (nm)
Xenon	39.0 ± 0.5a	7.8 ± 0.1a	180–1000
Ultraviolet	4.5 ± 0.1b	0.9 ± 0.0b	254

Means with different letters are significant different from each other at $P < 0.05$.

Table 2
Effect of etching solutions on the rate constant, initial degradation rate, half-life ($t_{1/2}$) and apparent quantum yield of congener 138 photocatalysis

TiO_2 (wt.%)	Purified	Etched	Rate constant (h^{-1})	Ini. degradation rate $\times 10^{-8}$(mol L^{-1} h^{-1})	$t_{1/2}$ (h)	Quantum yield $\times 10^{-4}$ (ϕ)
1	–[a]	G1	0.030	4.15	23.1	5.4
1	–	G2	0.063	8.68	10.1	11.3
1	–	G3	0.048	6.65	14.4	8.6
1	–	G4	0.039	5.37	17.9	7.0
5	–	G1	0.054	7.53	12.7	9.7
5	–	G2	0.116	16.11	5.9	20.8
5	–	G3	0.079	11.00	8.8	14.2
5	–	G4	0.066	9.17	10.5	11.8
1	+[b]	G1	0.040	5.59	17.2	7.2
1	+	G2	0.091	12.64	7.6	16.3
1	+	G3	0.069	9.50	10.1	12.4
1	+	G4	0.045	6.31	15.2	8.1
5	+	G1	0.041	5.72	16.8	7.4
5	+	G2	0.092	12.84	7.5	16.5
5	+	G3	0.072	10.00	9.6	12.9
5	+	G4	0.049	6.79	14.1	8.8

G1: 5 M NaOH; G2: 48% HF; G3: H_2SO_4/H_2O_2; G4: $HF/H_2O_2/NH_3$.
[a] – indicates without purification.
[b] + indicates with purification.

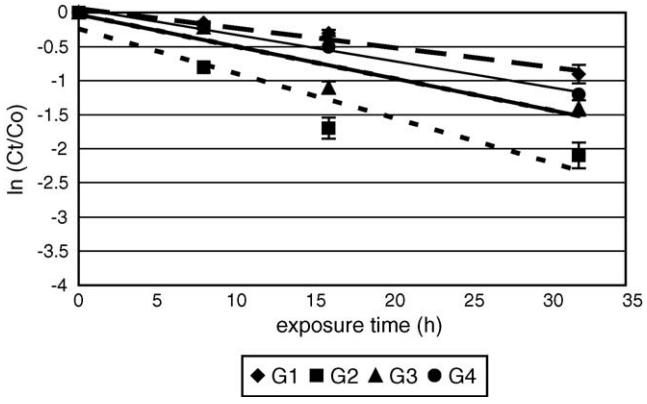

Fig. 5. Photocatalysis of PCB congener 138 using 1% unpurified TiO_2 on the support substrates etched by different solutions (G1: 5 M NaOH; G2: 48% HF; G3: H_2SO_4/H_2O_2; G4: $HF/H_2O_2/NH_3$).

either 1% or 5% TiO_2. Samples using HF etched support substrate and coated with 5% unpurified TiO_2 demonstrated the shortest half-life of congener 138 ($t_{1/2} = 5.9$ h) compared with the half-life of sample ($t_{1/2} = 23.1$ h) using NaOH (G1) and 1% unpurified TiO_2 (Table 2). The results of statistical analyses showed that the types of etching solution contributed significant impact on the initial photodegradation rates of congener 138. The initial reaction rates were in the sequence of the samples using G2 > G3 > G4 > G1 (Table 2). Although these four etching solutions demonstrated no difference on the XRD patterns of

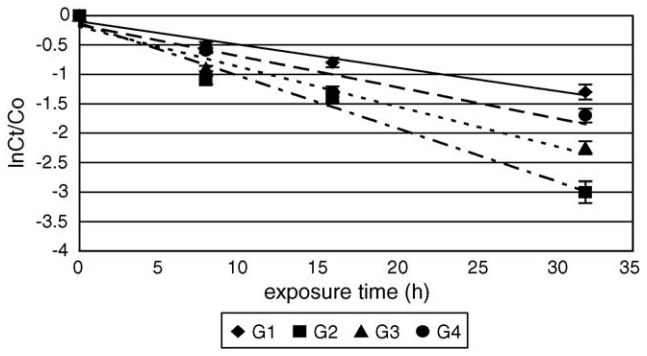

Fig. 6. Photocatalysis of PCB congener 138 using 5% unpurified TiO_2 on the support substrates etched by different solutions (G1: 5 M NaOH; G2: 48% HF; G3: H_2SO_4/H_2O_2; G4: $HF/H_2O_2/NH_3$).

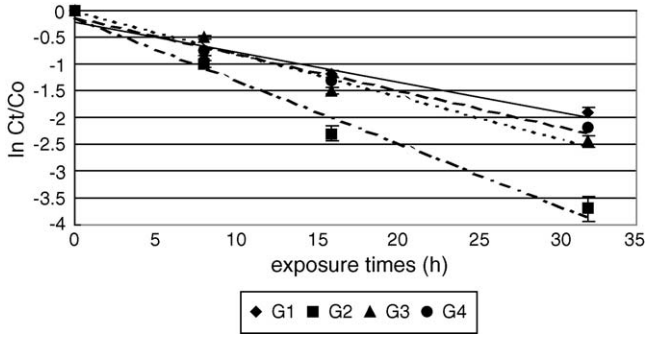

Fig. 7. Photocatalysis of PCB congener 138 using 1% purified TiO_2 on the support substrates etched by different solutions (G1: 5 M NaOH; G2: 48% HF; G3: H_2SO_4/H_2O_2; G4: $HF/H_2O_2/NH_3$).

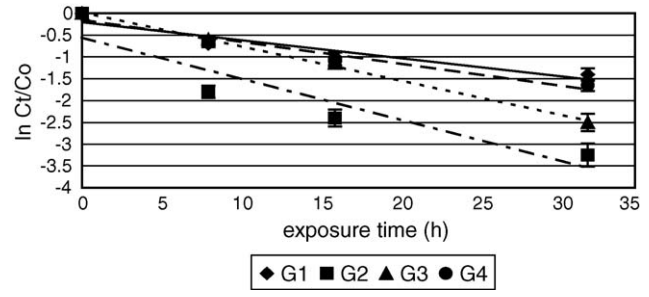

Fig. 8. Photocatalysis of PCB congener 138 using 5% purified TiO_2 on the support substrates etched by different solutions (G1: 5 M NaOH; G2: 48% HF; G3: H_2SO_4/H_2O_2; G4: $HF/H_2O_2/NH_3$).

Table 3
Effects of light sources and the concentrations of congener 138 on its rate constant, initial degradation rate, half-life ($t_{1/2}$) and apparent quantum yield

Light	Concentration (μmol L^{-1})	Rate constant (h^{-1})	Ini. degradation rate $\times 10^{-8}$ (mol L^{-1} h^{-1})	$t_{1/2}$ (h)	Quantum yield $\times 10^{-4}$ (ϕ)
Xe	2.8	0.063	17.64	11.0	11.3
Xe	1.4	0.083	11.62	8.4	14.9
Xe	0.28	0.094	2.63	7.4	16.8
UV	2.8	0.047	13.16	14.7	8.4
UV	1.4	0.054	7.56	12.8	9.6
UV	0.28	0.057	1.58	12.2	10.1

TiO_2 crystallization, their effects on the photocatalysis of congener 138 were significant. Studies showed that samples using the support substrate coated with 5% unpurified TiO_2 demonstrated higher photocatalytic rates than those using 1% TiO_2. However, samples using purified 1% or 5% TiO_2 did not show significant difference.

The initial degradation rates of congener 138 increased with the increasing of initial concentrations (0.28, 1.4, and 2.8 μmol L^{-1}) using either xenon or UV reactor (Table 3). The shortest half-life of congener 138 samples was 7.4 or 12.2 h using xenon or UV reactors, respectively. The effect of photoreactors on PCB photocatalysis was contributed by two factors. Firstly, the radiant energy of xenon lamp (38.9 mW cm^{-2}) was significantly higher than that of UV lamp (4.5 mW cm^{-2}). However, the half-lives of congener 138 after exposed to xenon or UV photoreactors were not inversely proportional to the energy. This phenomenon was caused by the other factor. Samples exposed to the UV reactor, mainly 254 nm radiation, had severe and more significant impact on the photocatalysis of congener 138. However, the wavelengths of visible light (380–780 nm) from xenon reactor showed less effect on the photocatalysis of congener 138. As a result, congener 138 exposed to the UV reactor had around 1.3–1.6 times longer half-life than those of samples exposed to xenon reactor.

Apparent quantum yields were used to compare the efficiency of congener 138 photocatalysis. The ranges of apparent quantum yield of congener 138 photocatalysis were from 2.1×10^{-3} to 5.4×10^{-4} (Table 2). Dullin and Mill [22] reported that the quantum yield of *p*-nitroanisole/pyridine was 5.7×10^{-3} [22]. The quantum yields of 1,2,4,7,8-pentachlorodibenzofuran and 1,2,3,4,7,8-hexachlorodibenzofuran were 1.3×10^{-2} and 6.9×10^{-3}, respectively reported by Choudhry et al. (1990) [33]. The quantum yields of these chlorinated xenobiotics were much lower than those of photosensitive chemicals such as nitrobenzaldehyde which was in the range of 0.45–1.46 reported by our previous investigation [34]. Dullin and Mill (1982) reported that sunlight actinometer such as nitrobenzaldehyde typically have the high value of quantum yield ($\phi > 0.5$) [22]. The result of comparison indicated that the chlorinated xenobiotics such as PCBs were less photosensitive and could be harder for photodegradation in natural environment.

To reach a more quantitative approach for chemical kinetics of congener 138 photocatalysis, the following model can be used to rationalize the Arrhenius equation [35]. The modeling equation listed below was applied to serve the purpose that allowed the reduction of the order of reaction law, ideally to pseudo-first order:

$$\text{Rate} = -A \exp(-E_a/RT) C_{PCB}$$

where A is the pre-exponential factor or frequency factor (1×10^{11}), E_a the activation energy (kJ mol^{-1}), R the 8.314×10^{-3} (kJ mol^{-1} K^{-1}), T the absolute temperature (K) and C_{PCB} is the concentration of PCB (mol L^{-1}).

The activation energy (E_a) for hydroxyl radical to initiate the dechlorination of congener 138 was 70.8 kJ mol^{-1}. The activation energy obtained here was a little less than the result reported by Murena et al. (2000) which had the activation energy of 92.8 kJ mol^{-1} [26].

3.4. Photocatalytic pathways of congener 138

To investigate the degradation pathway of congener 138 was a hard task due to its continuous degradation processes and formed high number of reaction intermediates with low concentrations. As a result in this study, lower chlorinated biphenyls were identified from the photocatalysis of congener 138 through dechlorination. Also, the concentrations of congener 138 decreased as the number of degraded intermediates increased. Mullin et al. (1984) [27] reported that the numbers and locations of chlorine atom on PCB congeners were the most important criteria for the evaluation of PCBs degradation [27]. In our study, PCB congeners 99 and 87 were detected after 30 min of light exposure through *meta*- and *para*-dechlorination (Fig. 9). In addition to congeners 99 and 87, congeners 66 and 49 were detected after 1 h of exposure. In addition to these four congeners, congeners 28 and 17 were identified mainly through *meta*-dechlorination after 2 h of light exposure. In addition to congeners 99, 87, 66, 49, 28, and 17 listed above, congeners 9 and 7 were detected after 3 h of exposure through *ortho*- and *para*-dechlorination. In this study, *meta*-dechlorination was the major photocatalytic pathway which confirmed the findings reported by Kuipers and Cullen (1999) [36] and Lepine et al. (1991) [37]. Xiu et al. (1999) also reported that congeners 118, 99, 97 and 87 were identified as the intermediates of congener 138 through *para*-dechlorination [38]. Miao et al. (1999) reported that congeners 99, 87, 66 were found as the degraded intermediates of congener 138 in hexane [11].

Majority of the dechlorination pathways of congener 138 identified in this study was through the removal of one chlorine ("de-monochlorination") including the formations of congeners 99, 87, 49, 28, 17, and 7. However, congeners 66, 28, and 9 were found possibly through the pathway of the removal of two

chlorine atoms ("de-dichlorination"). It was proposed that the intermediates between congeners 138 and 66 were congeners 118 and 85 through *ortho*- and *meta*-dechlorination, respectively (Fig. 9). The anticipated intermediates between congeners 99 and 28 were congener 74 (*ortho*-dechlorination) and congener 47 (*meta*-dechlorination). The suspected intermediates between congeners 49 and 9 were congener 31 (*ortho*-dechlorination) and congener 18 (*para*-dechlorination). These proposed intermediates were rapidly formed, degraded, and dissipated during the photocatalysis between sampling times. Therefore, the proposed intermediates had not been identified in GC analyses. The proposed intermediates (congeners 118, 85, 74, 47, 31, and 18) were indicated using dotted circles in Fig. 9.

The initial organic chlorine concentration of congener 138 was calculated as 58.97%. The concentration of organic chlorine was decreased as a function of irradiation time. The results verified that dechlorination was the major pathway of the photocatalysis of congener 138. Through the dechlorination of congener 138, the concentrations of chloride ion increased with the increasing of light exposure (Fig. 10). The results showed that the remaining of congener 138 was inversely proportional to the concentrations of chloride ion.

Dechlorination was the initial degradation mechanism of congener 138 as proved and discussed above. This finding can also be confirmed by comparing the bond energy in congener 138. The respective bond enthalpies of C–Cl, C–C, C–H, and C=C

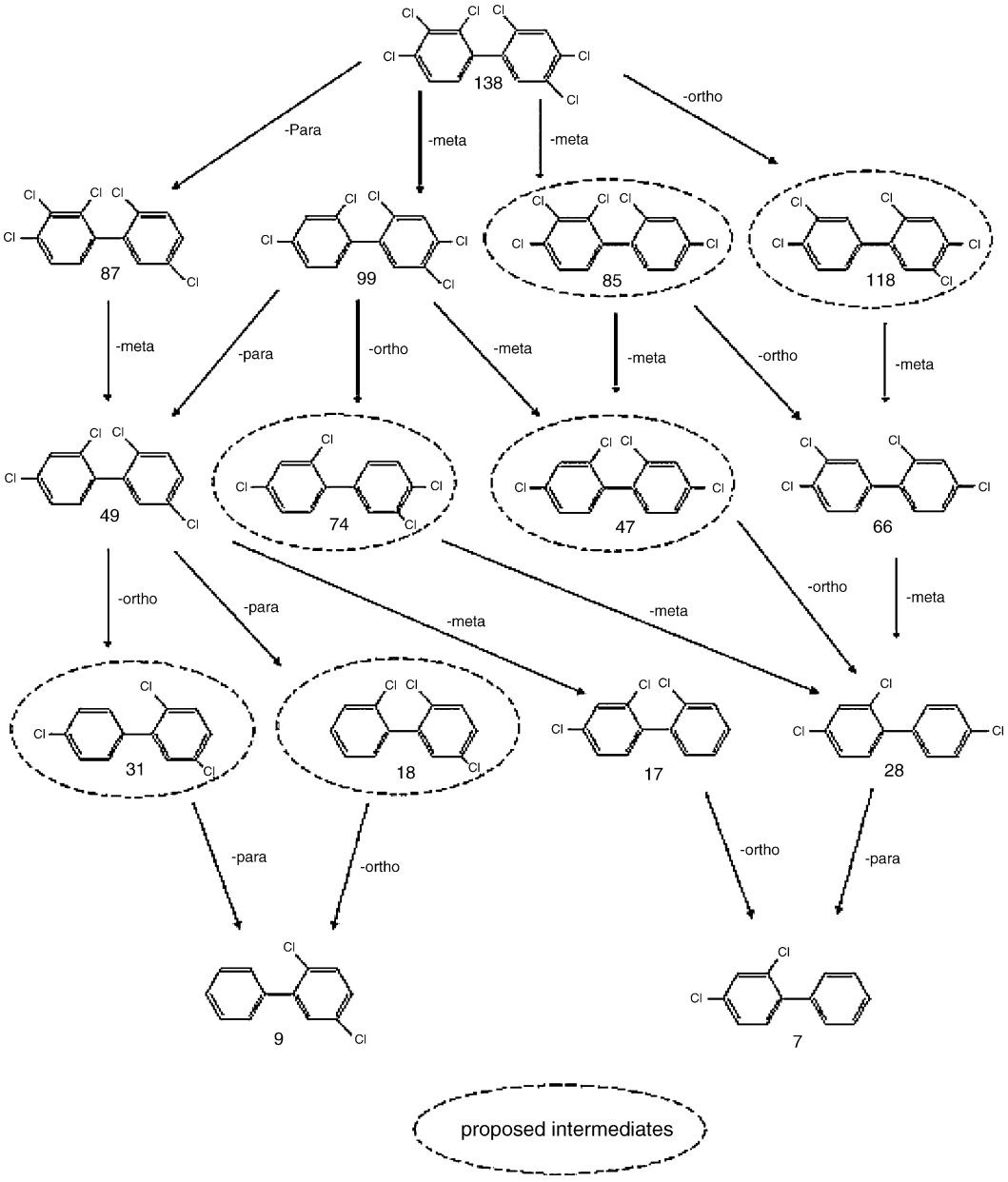

Fig. 9. Intermediates of PCB congener 138 photocatalysis (The locators *ortho*, *meta*, and *para* listed by arrows were the dechlorination locations of PCB congener 138).

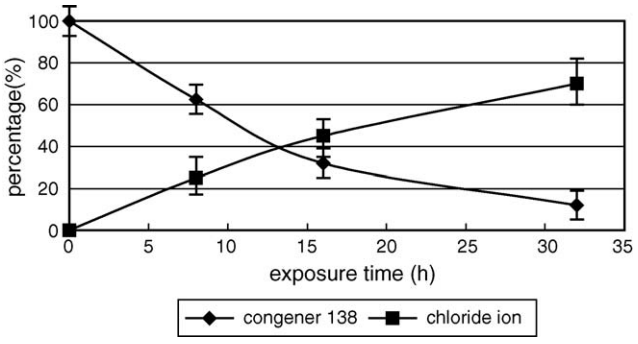

Fig. 10. Remaining of PCB congener 138 and the formation of chloride ion as a function of exposure time.

were 339, 348, 415, and 612 kJ mol^{-1} [25]. The enthalpy of C–Cl was the lowest energy compared to those of other covalent bonds in congener 138. Bond enthalpies can also be converted to the light wavelengths that are required to break particular covalent bonds. The wavelengths required to break C–Cl, C–C, C–H, and C=C were calculated as 353, 344, 288, and 195 nm, respectively using the following equations:

$$E = 6.02 \times 10^{23} \hbar\,(c/\lambda)$$

$$E = 1.196 \times 10^{5}/\lambda\,(\text{kJ Einstein}^{-1})$$

where $\hbar$ is the Plank constant (6.63×10^{-24} J s), c the speed of light in a vacuum (3.0×10^{8} m s^{-1}) and λ is the wavelength of light (nm).

4. Conclusions

Etching solutions used on support substrates were compared with no finding of difference on the XRD patterns of catalysts. However, samples using titanium(IV) tetraisopropoxide showed significant decrease in the relative intensities of both rutile and anatase phases. The support substrate etched by hydrofluoric acid and coated with 5% TiO_2 demonstrated the best photocatalytic result for congener 138. Because of the stronger light intensity of xenon reactor, samples exposed to that showed higher efficiency of photocatalysis compared with the samples using UV reactor. Initial reaction rates of congener 138 were not significantly different among samples using the catalysts with or without purification. Although the apparent quantum yields of congener 138 photocatalysis were similar to those of other chlorinated xenobiotics, they were much lower than that of nitrobenzaldehyde chemical actinometer which confirmed the low photosensitivity of congener 138. *Meta*-dechlorination was the most important degradation pathway for the photocatalysis of congener 138. Also, "de-dichlorination" (the removal of two chlorine atoms) was proposed for congeners 66, 28, and 9.

Acknowledgements

This research was supported by the National Science Council (NSC) of Taiwan, ROC under Grant NSC92-2211-E020-014. The authors thank its financial support.

References

[1] S. Sun, W.P. Inskeep, Sorption of nonionic organic compounds in soil-water systems containing a micelle-forming surfactant, Envrion. Sci. Technol. 29 (1995) 903–913.
[2] J. Wiegel, Q. Wu, Microbial reductive dehalogenation of polychlorinated biphenyls, FEMS Microbiol. Ecol. 32 (2000) 1–15.
[3] J.P. Woodyard, PCB detoxification technologies: a critical assessment, Environ. Prog. 9 (2) (1990) 131–135.
[4] F.L. Lepine, R. Masse, Degradation pathway of PCB upon gamma irradiation, Environ. Health Perspect. 89 (1990) 183–187.
[5] J. Hawari, A. Demeter, C. Greer, R. Samson, Acetone-induced photodechlorination of Aroclor 1254 in alkaline 2-propanol: probing the mechanism by thermolysis in the presence of di-*t*-butyl peroxide, Chemosphere 22 (1991) 1161–1174.
[6] J. Hawari, A. Demeter, R. Samson, Sensitized photolysis of polychlorobiphenyls in alkaline 2-propanol: dechlorination of Aroclor 1254 in soil samples by solar radiation, Environ. Sci. Technol. 26 (1992) 2022–2027.
[7] J.R. Bolton, S.R. Cater, in: G.R. Helz, R.G. Zepp, D.G. Crosby (Eds.), Aquatic and Surface Photochemistry, Lewis Publishers, Florida, 1994, p. 467.
[8] Y.J. Lin, G. Gupta, J. Baker, Photodegradation of polychlorinated biphenyl congeners using simulated sunlight and diethylamine, Chemosphere 31 (5) (1995) 3323–3344.
[9] Y.J. Lin, G. Gupta, J. Baker, Photodegradation of Aroclor 1254 using diethylamine and simulated sunlight, J. Hazard. Mater. 45 (1996) 259–264.
[10] J. Bachman, H.H. Patterson, Photodecomposition of the carbamate pesticide carbofuran: kinetics and the influence of dissolved organic matter, Environ. Sci. Technol. 33 (1999) 874–881.
[11] X.S. Miao, S.G. Chu, X.B. Xu, Degradation pathway of PCBs upon UV irradiation in hexane, Chemosphere 39 (10) (1999) 1639–1650.
[12] M.I. Stefan, J.R. Bolton, Reinvestigation of the acetone degradation mechanism in diluted aqueous solution by the UV/H_2O_2 process, Environ. Sci. Technol. 33 (1999) 870–873.
[13] N. Serpone, E. Borgarello, R. Harris, P. Cahill, M. Borgarello, Photocatalysis over TiO_2 supported on a glass substrate, Solar Energy Mater. 14 (1986) 121–127.
[14] S. Sampath, H. Uchida, H. Yoneyama, Photocatalytic degradation of gaseous pyridine over zeolite-supported titanium dioxide, J. Catal. 149 (1994) 189–194.
[15] L.W. Miller, M.I. Tejedor, M.A. Anderson, Titanium dioxide-coated silica waveguides for the photocatalytic oxidation of formic acid in water, Environ. Sci. Technol. 33 (1999) 2070–2075.
[16] K.Y. Jung, S.B. Park, Enhanced photoactivity of silica-embedded titania particles prepared by sol-gel process for the decomposition of trichloroethylene, Appl. Catal. B 25 (2000) 249–256.
[17] I.K. Konstantinou, T.M. Sakellarides, V. Sakkas, T.A. Albanis, Photocatalytic degradation of selected s-triazine herbicides and organophosphorus insecticides over aqueous TiO_2 suspensions, Environ. Sci. Technol. 35 (2001) 398–405.
[18] S. Parra, J. Olivero, C. Pulgarin, Relationships between physicochemical properties and photoreactivity of four biorecalcitrant phenylurea herbicides in aqueous TiO_2 suspension, Appl. Catal. B 36 (2002) 75–85.
[19] Y.J. Lin, L.S. Teng, A. Lee, Y.L. Chen, Effect of photosensitizer diethylamine on the photodegradation of polychlorinated biphenyls, Chemosphere 55 (6) (2004) 879–884.
[20] W. Chu, Photodechlorination mechanism of DDT in UV/surfactant system, Environ. Sci. Technol. 33 (1998) 421–425.
[21] Y.J. Lin, C. Lin, K.J. Yeh, A. Lee, Photodegradation of the herbicides butachlor and ronstar using natural sunlight and diethylamine, Bull. Environ. Contam. Toxicol. 64 (6) (2000) 780–785.
[22] D. Dullin, T. Mill, Development and evaluation of sunlight actinometers, Environ. Sci. Technol. 16 (1982) 815–820.
[23] R.P. Schwarzenbach, P.M. Gschwend, D.M. Imboden, Environmental Organic Chemistry, John Wiley and Sons, New Jersey, 2003, p. 20.
[24] A. Fernandz, G. Lassaletta, V.M. Jimenez, A. Justo, A.R. Gonzalez-Elipe, J.M. Herrmann, H. Tahiri, Ait-Ichou, Preparation and characteri-

zation of TiO_2 photocatalysts supported on various rigid supports (glass, quartz and stainless steel). Comparative studies of photocatalytic activity in water purification, Appl. Catal. B 7 (1995) 49–63.
[25] T. Torimoto, S. Ito, S. Kuwabata, H. Yoneyama, Effects of adsorbents used as supports for titanium dioxide loading on photocatalytic degradation of propylazimide, Environ. Sci. Technol. 30 (1996) 1275–1281.
[26] F. Murena, E. Schioppa, F. Gioia, Catalytic hydrodechlorination of a PCB dielectric oil, Environ. Sci. Technol. 34 (2000) 4382–4385.
[27] M.D. Mullin, C.M. Pochini, S. McCrindle, M. Romkes, S. Safe, L.M. Safe, High-resolution PCB analysis: synthesis and chromatographic properties of all 209 PCB congeners, Environ. Sci. Technol. 18 (1984) 468–476.
[28] H. Gao, W. Lu, Q. Chen, Characterization of titanium silicalite-1 prepared from aqueous $TiCl_3$, Micropor. Mesopor. Mater. 34 (2000) 307–315.
[29] E.D. Nelson, L.L. McConnell, J.E. Baker, Diffusive exchange of gaseous polycyclic aromatic hydrocarbons and polychlorinated biphenyls across the air-water interface of the Chesapeake Bay, Environ. Sci. Technol. 32 (1998) 912–919.
[30] B. Renard, J. Barbier Jr., D. Duprez, S. Durecu, Catalytic wet air oxidation of stearic acid on cerium oxide supported noble metal catalysts, Appl. Catal. B 55 (2005) 1–10.
[31] A. Haarstrick, O.M. Kut, E. Heinzle, TiO_2-assisted degradation of environmentally relevant organic compounds in wastewater using a novel fluidized bed photoreactor, Environ. Sci. Technol. 30 (1996) 817–827.
[32] R.A. Doong, W.H. Chang, Photoassisted titanium dioxide mediated degradation of organophosphorus pesticides by hydrogen peroxide, J. Photochem. Photobiol. A 107 (1997) 239–244.
[33] G.G. Choudhry, M. Foga, G. Webster, Quantum yield of the direct phototransformation of 1,2,4,7,8-penta- and 1,2,3,4,7,8-hexachlorodibenzofuran in aqueous acetonitrile and their sunlight half-lives, Toxicol. Environ. Chem. 26 (1990) 181–195.
[34] Y.J. Lin, A. Lee, L.S. Teng, H.T. Lin, Effect of experimental factors on nitrobenzaldehyde photoisomerization, Chemosphere 48 (2002) 1–8.
[35] B. Wehrli, in: W. Stumm (Ed.), Aquatic Chemical Kinetics, John Wiley and Sons, Inc., New York, 1990, p. 319.
[36] B. Kuipers, W.R. Cullen, Reductive dechlorination of nonachlorobiphenyls and selected octachlorobiphenyls by microbial enrichment cultures, Environ. Sci. Technol. 33 (1999) 3579–3585.
[37] F.L. Lepine, S.M. Milot, N.M. Vincent, D. Grave, Photochemistry of higher chlorinated PCBs in cyclohexane, J. Agric. Food Chem. 39 (1991) 2053–2056.
[38] S.M. Xiu, G.C. Shao, B.X. Xiao, Degradation pathways of PCBs upon UV irradiation in hexane, Chemosphere 39 (1999) 1639–1650.